(7) M. Gerloch and P. N. Quested, *J. Chem. Soc. A*, 2308 (1971).
(8) M. Gerloch and I. Morgenstern-Badarau, *J. Chem. Soc., Dalton Trans.*, 1619 (1977).
(9) M. Gerloch and R. F. McMeeking, *J. Chem. Soc., Dalton Trans.*, 2443 (1975).
(10) J. Ferguson, *Prog. Inorg. Chem.*, **12**, 159 (1970).
(11) D. A. Cruse and M. Gerloch, *J. Chem. Soc., Dalton Trans.*, 1613 (1977).
(12) M. Gerloch, R. F. McMeeking, and A. M. White, *J. Chem. Soc., Dalton Trans.*, 2452 (1975).
(13) P. D. W. Boyd, J. E. Davies, and M. Gerloch, *Proc. Soc. London, Ser. A*, **360**, 191 (1978).
(14) J. E. Davies and M. Gerloch, manuscript in preparation.

Contribution from the University Chemical Laboratories, Cambridge CB2 1EW, United Kingdom, and the Laboratoire de Spectrochimie des Elêments de Transition, Université de Paris Sud, 91405 Orsay, France

Magnetic and Spectral Properties of Chloroaqua[2,6-diacetylpyridine bis(semicarbazone)]iron(II) and Diaqua[2,6-diacetylpyridine bis(semicarbazone)]nickel(II): Ligand Fields and Bonding in Pentagonal-Bipyramidal Complexes

MALCOLM GERLOCH* and IRÈNE MORGENSTERN-BADARAU

Received January 8, 1979

Principal crystal susceptibilities throughout the temperature range 10–300 K have been measured for the complexes $[Ni(DAPSC)(H_2O)_2]^{2+}(NO_3^-)_2 \cdot H_2O$ and $[Fe(DAPSC)Cl,H_2O]^+Cl^- \cdot 2H_2O$, where DAPSC is 2,6-diacetylpyridine bis(semicarbazone). The unpolarized, single-crystal transmission spectra have been recorded in the UV, visible, and near-IR regions. The complete crystal magnetic properties and spectral features of the nickel complex have been reproduced simultaneously within the angular overlap model (aom) the parameters of which reflect the longer Ni–O(keto) bond lengths observed relative to Co–O in the analogous cobalt complex. The magnetism of the iron system is quantitatively reproduced by a similar model and reflects the similarity of the Fe–O(keto) bond lengths with respect to those in the cobalt complex. A detailed discussion of the equivalent orbital diagrams established by the ligand field analyses of the iron(II), cobalt(II), and nickel(II) complexes is presented, from which a rationale of the first-coordination-shell bond lengths in these and the analogous copper(II) molecules emerges.

Introduction

In the preceding paper[1] we reported a study of the spectral and single-crystal magnetic properties of two formally pentagonal-bipyramidal cobalt(II) complexes involving the 2,6-diacetylpyridine bis(semicarbazone) ligand (DAPSC). The results were interpreted within an angular overlap model (aom), parameters referring to the local σ- and π-bonding interactions between the central metal atom and each ligand. We present here a study of the spectral and single-crystal magnetic properties of two other members of this series in order to complement discussions by Palenik and Wester[2-5] upon trends revealed by their X-ray structural analyses of these species. The complexes studied here are $[Fe(DAPSC)Cl,H_2O]^+Cl^- \cdot 2H_2O$ and $[Ni(DAPSC)(H_2O)_2]^{2+}(NO_3^-)_2 \cdot H_2O$. Again the efficacy of the angular overlap model and of our application of it to the magnetic and spectral properties of low-symmetry molecules[6] is of particular interest and we show that not only are the experimental magnetism and spectroscopy quantitatively reproduced by the technique but also they are reproduced in a manner which directly relates to the bonding and structure in this series of complexes.

Experimental Section

The 2,6-diacetylpyridine bis(semicarbazone) ligand (DAPSC) was prepared as described previously.[1] The complex of stoichiometry DAPSC, $FeCl_2$, $3H_2O$ was prepared in a manner similar to that[1] of the cobalt analogue, from iron(II) chloride, except that crystallization of the complex $[Fe(DAPSC)Cl,H_2O]^+Cl^- \cdot 2H_2O$ took place directly from the concentrated solution without previous dissolution in water. The solution is somewhat unstable with respect to air and water but yields black platelike crystals which are stable to the atmosphere. Satisfactory C, N, H, and Cl analyses are reported in Table I.

Crystals of the nickel complex DAPSC, $Ni(NO_3)_2$, $3H_2O$ were prepared as for the analogous cobalt compound. However, two different crystal forms are produced: one, yellow-green, was found to have the unit cell dimensions listed by Palenik[2] for the desired complex; the other, forming green rods, was found to crystallize in a triclinic cell with dimensions $a = 7.04$ Å, $b = 12.49$ Å, $c = 13.44$ Å, $\alpha = 119.5°$, $\beta = 107.2°$, and $\gamma = 75.89°$. The cocrystallization of the two forms, while in no way preventing our obtaining good crystals of the desired crystals, is undoubtedly responsible for the less good analyses reported in Table I. That the analytical figures are nevertheless fair suggests that the stoichiometry of the triclinic form is similar to that of the monoclinic one. Further study of the triclinic crystals is currently under way.

Susceptibility measurements of the iron and nickel monoclinic crystals, isomorphous with the corresponding cobalt complexes, were performed throughout the temperature range 10–300 K, as described previously.[1] Duplicate measurements from different crystals agree to better than 3%. Values for the monoclinic ϕ angles, calculated from the equation[7]

$$\sin^2(\beta - 90° - \phi) = (\chi_{a'} - \chi_1)/(\chi_2 - \chi_1)$$

were determined as −25 and −55 °C for the iron and nickel crystals, respectively.

After the correction for a gross diamagnetic susceptibility of -170×10^{-6} cgsu, determined for the DAPSC, $ZnCl_2$, $3H_2O$ complex, the interpolated, principal crystal susceptibilities of the two complexes are collected in Table II.

The electronic absorption transmission spectra have been recorded for crystals of the pure nickel complex and for crystals of the zinc complex doped with ca. 10% iron. The spectrum of the nickel compound, recorded at ca. 80 K by using a Cary 14 spectrometer, is reproduced in Figure 1. No significant spectral features have been observed for the iron complex apart from the onset of a charge-transfer region above 20 000 cm^{-1}.

Discussion

A. Fitting Spectral and Magnetic Properties. Using the same techniques as in the earlier paper[1] and as reported in detail elsewhere,[8] we performed calculations of eigenvalues, eigenvectors, and magnetic properties within the complete

* To whom correspondence should be addressed at the University Chemical Laboratories.

0020-1669/79/1318-3225$01.00/0

Table I. Elemental Analysis

	% C		% H		% N		% Cl	
	calcd	found	calcd	found	calcd	found	calcd	found
DAPSC, $FeCl_2$, $2H_2O$	28.82	28.70	4.58	4.73	21.40	21.70	15.50	15.76
DAPSC, $Ni(NO_3)_2$, $3H_2O$	25.69	26.99	4.09	4.48	24.53	23.0		

Table II. Observed Interpolated, Principal Crystal Susceptibilities χ (cgsu $\times 10^4$; 1 cgsu = $4\pi \times 10^{-6}$ m^3 mol^{-1}) and Mean Moments (μ_B)

	$[Ni(DAPSC)(H_2O)_2]^{2+}$-$(NO_3^-)_2 \cdot H_2O$				$[Fe(DAPSC)Cl,H_2O]^+Cl^- \cdot 2H_2O$			
T/K	χ_1	χ_2	χ_3	$\bar{\mu}$	χ_1	χ_2	χ_3	$\bar{\mu}$
20	390	692	460	2.87	570	3080	750	4.84
40	248	360	284	3.08	462	1530	560	5.22
60	180	240	198	3.14	360	910	423	5.20
80	138	175	146	3.13	290	628	330	5.16
100	112	138	118	3.13	245	480	274	5.16
120	95	112	98	3.12	213	393	235	5.18
140	82	96	84	3.13	187	326	202	5.17
160	71	84	74	3.12	168	280	178	5.17
180	64	74	65	3.12	150	248	160	5.17
200	58	66	59	3.12	138	217	144	5.16
220	52	60	54	3.12	126	194	132	5.15
240	48	55	49	3.12	116	172	120	5.11
260	44	52	45	3.13	108	158	112	5.12
280	42	48	43	3.15	100	146	103	5.11
300	40	46	41	3.19	94	136	96	5.11

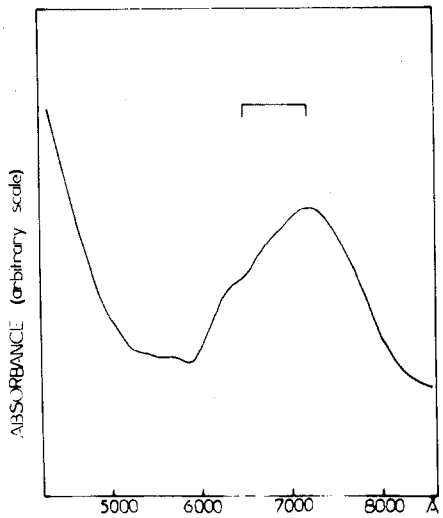

Figure 1. Transmission spectrum of $[Ni(DAPSC)(H_2O)]^{2+}$-$(NO_3^-)_2 \cdot H_2O$ at ca. 80 K.

spin-triplet basis, $^3P + {}^3F$, of the d^8 configuration for nickel(II) and within the ^5D manifold of d^6 for iron(II). Donor atoms were placed at coordinates given by the relevant X-ray analyses[2-5] and the parameter list following refers to the numbering scheme given in Figure 2. Donor atoms N2 and N5 are presumed chemically equivalent as, initially at least, are O1 and O2. The axial ligands—both H_2O for the nickel complex, but one H_2O and one Cl for the iron one—are assigned shared parameters, as in the previous paper[1] and in recognition of the approximate holohedral relationship between them. We therefore consider the ligand field parameters: for N1 e_σ, $e_{\pi\perp}$, $e_{\pi\parallel}$ (expected = 0), for N2,5 e_σ, $e_{\pi\perp}$, $e_{\pi\parallel}$ (expected = 0), for O1,2 e_σ, $e_{\pi\perp}$, $e_{\pi\parallel}$, for $^1/_2(Cl + H_2O)$ e_σ, $e_{\pi av}$, where $\perp$ and $\parallel$ refer to π bonding perpendicular and parallel to the pentadentate plane. Calculations thus involve 11 aom parameters plus B, ζ, and k for interelectron repulsion, spin–orbit coupling, and orbital reduction effects. Some calculations for the nickel complex were performed in which the keto groups O1 and O2 were not presumed equivalent and are referred to later.

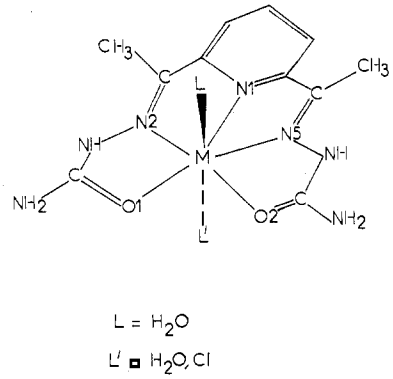

Figure 2. Numbering of DAPSC donor atoms.

$[Ni(DAPSC)(H_2O)_2]^{2+}(NO_3^-)_2 \cdot H_2O$. The spectrum of the nickel complex is characterized by a broad band at ca. 13 900 cm^{-1} with a shoulder at ca. 15 600 cm^{-1}. There is some indication of a weak, broad feature at 7000–8000 cm^{-1} but it is not well resolved in our spectrum. No other details are observable apart from the intense tail at energies above ca. 21 000 cm^{-1}.

In the previous paper,[1] it was demonstrated that for the cobalt analogues of the present compounds the transitions from ^4F to ^4P levels *all* lie in the region 16 000–18 000 cm^{-1} with the ^4F manifold split up to ca. 12 000 cm^{-1}. In particular, no spin-allowed d–d transitions occur in the "charge-transfer" region at and above 21 000 cm^{-1}. By analogy, for the present nickel system, we may consider the features at 13 000–16 000 cm^{-1} as belonging entirely to the transitions $^3F \rightarrow {}^3P$, again with the high-energy region above 21 000 cm^{-1} being "charge transfer" in nature. We find, however, that such an assignment is quantitatively unacceptable. Even an approximate reproduction of the 13 000–16 000-cm^{-1} spectral region in this way requires very low values for the Racah B parameter and e_σ values for all ligands no more than ca. 2000 cm^{-1}. Further, such values are incompatible with the observed magnetic properties. Attempts to assign components of the ^3P at ca. 15 000 cm^{-1} and higher than ca. 21 000 cm^{-1} simultaneously are also inept, especially because a splitting of the ^3P manifold by 6000 cm^{-1} or more requires enormous values for all e_σ parameters. Therefore, we conclude that the spectrum of the nickel complex is not to be assigned in the same way as the cobalt one.

By contrast, there is no problem with assignments which place the $^3F \rightarrow {}^3P$ transitions all above 21 000 cm^{-1}, but restrictions on aom parameter values are exacted by requiring two transitions within the ^3F manifold at 13 900 and 15 600 cm^{-1}. In particular, few combinations of e parameters will reproduce the shoulder at 15 600 cm^{-1}. Suitable values were estimated initially by reference to the published bond lengths in the nickel and cobalt analogues, some of which are reproduced in Table III. On the replacement of cobalt by nickel, M–N bond lengths decrease,[2-4] but only very little; metal–water distances decrease rather more. Accordingly, we use the "best fit" parameter set established[1] for the $[Co(DAPSC)(H_2O)_2]^{2+}$ complex with values for $e_\sigma(N)$ and $e_\sigma(H_2O)$ increased somewhat. This helps to raise the calculated energy of the highest components of ^3F; however, these changes alone are not able to raise these energies above ca. 13 500 cm^{-1} and reproduction of the shoulder at ca. 15 600 cm^{-1} *uniquely*

Table III. Summary of First-Coordination-Shell Bond Lengths (Å) in DAPSC Complexes[2-5]

bond	$Fe(Cl/H_2O)^a$	$Co(Cl/H_2O)$	$Co(H_2O)_2$	$Ni(H_2O)_2$	$Cu(H_2O)_2$
M-N1	2.220	2.189	2.192	2.060	2.265
M-N2	2.229	2.196	2.211	2.222	2.258[b]
M-N5	2.215	2.186	2.205	2.108	2.258
M-O1	2.192	2.165	2.201	2.478	2.350
M-O2	2.175	2.186	2.154	2.216	2.350
M-O3(aq)	2.153	2.137	2.176	2.048	1.922
M-O4(aq)			2.116	2.090	1.922
M-Cl	2.507	2.476			

[a] Abbreviation refers to the axial ligands in each case. [b] N2 and N5, O1 and O2, and O3 and O4 are crystallographically related by a diad in the copper complex.

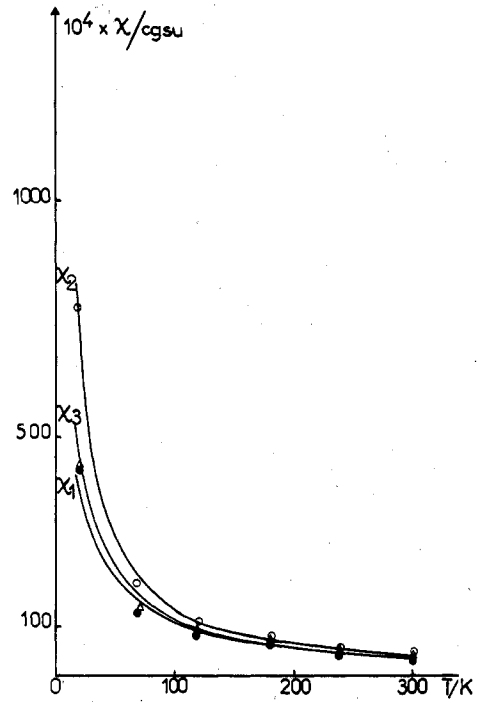

Figure 3. $[Ni(DAPSC)(H_2O)_2]^{2+}(NO_3^-)_2 \cdot H_2O$. Comparison of principal crystal susceptibilities from experiment (full lines) and those calculated with the parameters given in Table XI (calculated ϕ = −59°; observed ϕ = −55°).

requires a dramatic reduction in the e parameters associated with the keto groups. The magnetic properties are not markedly sensitive to these parameters, once all other parameter values have been set near those established for the cobalt compounds, nor is the spectrum especially sensitive to the σ-bonding parameter of the oxygen donors, though a reduction with respect to the cobalt parameters is preferred. The predominant feature is the magnitude of $e_{\pi\perp}(O)$ which must be reduced from the "cobalt value" of ca. 2000 to 100 cm^{-1} or less in the nickel complex. The much reduced e parameters for the Ni–O interaction clearly reflect the markedly longer bonds as compared with those in the cobalt system (Table III) and are discussed further below. The two Ni–O bonds are quite unequal, however, and, despite the associated increase in parameterization, we have attempted to investigate this by ascribing separate e values to the two keto groups. This was done by assigning an e_σ value of 1000 cm^{-1} to the longer Ni–O bond and 2000 cm^{-1} to the shorter one. At the same time, $e_{\pi\perp}$ was set at zero for the long bond and at various values from 0 to 2000 cm^{-1} for the shorter one. As before, the magnetic properties are insensitive to these changes while the variation in $e_{\pi\perp}$ for the short Ni–O bond essentially only affects the spectral shoulder at 15600 cm^{-1}. The calculated energy of this band increases as $e_{\pi\perp}(O)$ decreases and we obtain the (expected) result that best agreement occurs when the average value of $e_{\pi\perp}(O)$ is close to the value taken when the two oxygen atoms are presumed equivalent. In effect the present model is incapable of distinguishing these two oxygen donors in this nickel complex.

Table IV. $[Ni(DAPSC)(H_2O)_2]^{2+}(NO_3^-)_2 \cdot H_2O$ Summary of Simultaneous Best Fits to Spectrum and Magnetism (Energies in cm^{-1}), Corresponding to the Parameter Set Given in Table XI

calcd eigenvalues	obsd spectral peaks
25 660	>22 000
24 010	
23 420	
15 460	15 600 sh
14 510	13 900
13 620	
9 550	
9 350	
3 980	
0 (av over spin triplet)	

Table V. Molecular Susceptibilities[a] Calculated with the Parameters Given in Table XI

	$[Ni(DAPSC)(H_2O)_2]^{2+}(NO_3^-)_2 \cdot H_2O$			$[Fe(DAPSC)Cl,H_2O]^+Cl^- \cdot 2H_2O$		
T/K	K_1	K_2	K_3	K_1	K_2	K_3
300	36.5	37	44	102	106	130
240	45	46	55	125	130	167
180	60	61	73	162	168	231
120	88	90	110	231	240	367
70	148	150	192	354	366	703
20	437	443	773	594	609	3378

[a] cgsu × 10^4.

Table VI. Orientation of the Principal Molecular Susceptibilities (deg) at 150 K

	X	Y	Z
K_1	164.9	105.2	89.8
K_2	74.9	164.9	90.0
K_3	89.8	89.9	0.3

Table VII. Direction Cosines

	a	b	c′
X	−0.2997	−0.7977	0.5233
Y	0.4132	−0.6029	−0.6825
Z	0.8599	0.0117	0.5104

Despite some degree of parameter correlation, as discussed in the previous paper, the "best fit" parameter values given in Table XI reproduce the spectrum satisfactorily (Table IV) and yield calculated principal crystal susceptibilities in agreement with experiment to within ca. 5% over the 10–300 K temperature range (Figure 3). The molecular susceptibilities associated with these calculations reflect the approximate fivefold axial molecular symmetry with a secondary twofold perturbation in the same manner as found for the cobalt analogues except that, here, the "unique" susceptibility K_3, lying nearly perpendicular to the pentagon plane, is the

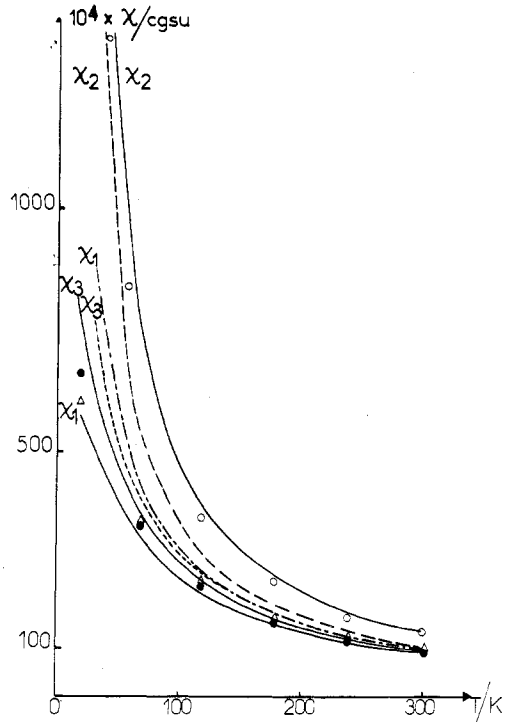

Figure 4. $[Fe(DAPSC)Cl,H_2O]^+Cl^-\cdot 2H_2O$. Comparison of principal crystal susceptibilities from experiment (full lines) and those calculated with the parameters given in Table XI (calculated $\phi = -39°$; observed $\phi = -25°$). Also shown (broken lines) are susceptibilities calculated with parameters from Table XI appropriate to the nickel complex.

Table VIII. Calculated Eigenvalues (cm^{-1}) for $[Fe(DAPSC)Cl,H_2O]^+Cl^-$ with the Parameter Set Given in Table XI[a]

8535, 3750, 2320, 610, 0

[a] Values averaged over spin quintet.

largest. The orientations of these principal molecular susceptibilities, shown in Table V, vary by less than 0.5° over the temperature range, and at 150 K are given in Table VI, where the molecular frame X, Y, and Z, defined with Z perpendicular to the plane and X parallel to Ni–N1, is oriented with respect to the crystallographic axes by the direction cosines (Table VII).

$[Fe(DAPSC)Cl,H_2O]^+Cl^-\cdot 2H_2O$. The spectrum of this complex was featureless from ca. 6000 to 20 000 cm^{-1}, except for some indication of a very broad absorption at less than 10 000 cm^{-1}. At ca. 20 000 cm^{-1} we observe the onset of a typical charge-transfer tail. Accordingly, our analysis for the iron complex is based upon the reproduction of the crystal magnetism only. The bond lengths in the iron and cobalt chloroaqua complexes (Table III) are closely similar and the principal crystal susceptibilities of the iron complex, calculated by using the parameter set of the analogous cobalt molecule but with suitably optimized values of B, ζ, and k, as given in Table XI are in excellent agreement with experiment. The quality of the fit is rather sensitive to $e_\pi(O)$, giving this value as $+2000 \pm 150$ cm^{-1}. By contrast, the magnetic properties calculated from the parameter set appropriate to the nickel complex, also suitably optimized with respect to B, ζ, and k, disagree markedly with experiment (Figure 4), reflecting the very different Fe–O1,2 and Ni–O1,2 bond lengths. The calculated "best fit" spectrum is given in Table VIII.

The orientations of the molecular tensors (essentially independent of temperature) are similar in the iron and nickel complex, details being collected in Table V. The orientation of the molecular magnetic tensor at 120 K is given in Table IX, with respect to the direction cosines (Table X).

Table IX. Orientation of the Molecular Magnetic Tensor at 120 K (deg)

	X	Y	Z
K_1	15.0°	75.1	91.5
K_2	75.9	160.1	103.8
K_3	85.1	102.9	13.8

Table X. Direction Cosines

	a	b	c'
X	0.0320	0.9979	0.0558
Y	0.8958	−0.0038	−0.4446
Z	−0.4434	0.0642	−0.8940

Table XI. Summary of "Best Fit" Parameter Sets Used to Reproduce Spectral and Magnetic Data on DAPSC Complexes of Iron(II), Cobalt(II), and Nickel(II) (Energies in cm^{-1})

parameter		$Fe(Cl/H_2O)$[b]	$Co(Cl/H_2O)$[c]	$Co(H_2O)_2$[c]	$Ni(H_2O)_2$[b]
N1	e_σ	4400	4500	4500	4800
	$e_{\pi\parallel}$	0	0	0	0
	$e_{\pi\perp}$	200	200	200	200
N2,5	e_σ	3500	3500	3500	4200
	$e_{\pi\parallel}$	0	0	0	0
	$e_{\pi\perp}$	1000	1000	1000	1000
O1,2	e_σ	2500	2500	2500	2000
	$e_{\pi\parallel}$	400	400	400	0
	$e_{\pi\perp}$	2000	2000	2000	100
axial[a]	e_σ	4000	4000	4500	5200
	$e_{\pi av}$	800	800	400	500
B		750	800	800	850
ζ		400	500	500	300
k		0.6	0.5	0.5	0.7

[a] Refers either to each water interaction in the diaqua complexes or to the average of chlorine and water interactions in the chloroaqua species. [b] This paper. [c] Preceding paper.

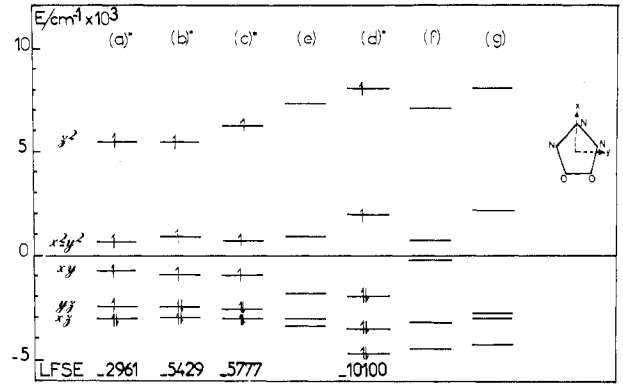

Figure 5. Orbital diagrams for DAPSC complexes of iron(II), cobalt(II), and nickel(II). LFSE's (in cm^{-1}) are shown with each diagram. Orbital labeling (corresponding to ≳95% pure) corresponds to the axis frame shown in the inset. All calculations were performed with vanishing spin–orbit coupling: (a) for $Fe(Cl/H_2O)$; (b) for $Co(Cl/H_2O)$; (c) for $Co(H_2O)_2$; (d) for $Ni(H_2O)_2$; (e) for $Ni(H_2O)_2$ parameters, except $e_{\pi\perp}(O) = 2000$ cm^{-1} and $e_{\pi\parallel}(O) = 400$ cm^{-1}; (f) for $Co(H_2O)_2$ parameters, except $e_{\pi\perp}(O) = 100$ cm^{-1} and $e_{\pi\parallel}(O) = 0$; (g) for $Ni(H_2O)_2$ parameters, except $e_\sigma(O) = 1000$ cm^{-1}. An asterisk marks the orbital diagrams corresponding to the parameter sets given in Table XI.

B. Orbital Diagrams and a Commentary on the Bonding in These Pentagonal-Bipyramidal Complexes. In Table XI are collected the "best fit" parameter values for the four molecules discussed in this and the preceding paper.[1] Corresponding to these parameter sets, the one-electron eigenvalues, for simplicity calculated without spin–orbit coupling, are presented graphically in Figure 5, the predominant cubic parentage of each orbital in the figure being indicated. Also shown are the

ligand field stabilization energies (LFSE) for each molecular ion calculated with respect to the usual d orbital baricenters.

The small differences in the orbital diagrams for the d^6 and d^7 species arise from the greater π-donating role of the axial chlorines relative to water. However, the diagram for the nickel complex is very different. Two subsidiary calculations, both based upon the $[Co(DAPSC)(H_2O)_2]^{2+}$ entity, involve changing (Figure 5g) only the σ-bonding parameters to correspond to the nickel complex and (Figure 5e) only the π parameters. The results show that the difference between the orbital energies of the cobalt and nickel species is dominated by the change in π bonding on lengthening the M–O distances. We have already mentioned that changes in $e_\sigma(O)$ are relatively unimportant so far as the spectral and magnetic properties are concerned. An increase of ca. 3000 cm^{-1} in the ligand field stabilization energy (LFSE) occurs on passing from cobalt to nickel while an extra electron housed within the cobalt orbital stack would contribute ca. 1000 cm^{-1} increase in LFSE. Hence the decrease in π bonding from the Ni–O interaction increases the LFSE by ca. 2000 cm^{-1}. However, we do not suggest this as a driving force for the "distortion" observed in the nickel complex, for a similar argument would favor the same distortion occurring in the d^7 cobalt species. Also shown in Figure 5 is the orbital diagram for the nickel compound calculated with $e_\sigma(O) = 1000$ cm^{-1} rather than 2000 cm^{-1}. The magnetism is only trivially affected by this change and the spectrum only altered in the 4000–5000-cm^{-1} region. Nevertheless, the orbital diagram changes significantly, although our remarks about relative LFSE are substantially unaffected.

A *rationale* for the bonding in these species emerges from a recognition of the *acceptor* properties of the relevant orbitals as deduced from their equilibrium electron populations. The tautology implied is analogous to that involved in the well-known "synergic" description of M–L back-bonding: in effect we consider the end product of an imaginary, self-consistent computation. Now the xy orbital of the metal interacts more with the oxygen σ-donor orbitals than with the nitrogen σ lobes: the $x^2 - y^2$ metal orbital overlaps better with Nσ than Oσ. Accordingly, on replacing cobalt with nickel, the xy orbital houses two electrons rather than one and so we expect the acceptor property of this orbital to decrease. In turn the M–O bonds lengthen, as observed (Table III).[10] The π-bonding role of these oxygen donors is accordingly greatly reduced and is manifest in the spectral splitting. Conversely, the spectrum provides the probe by which these effects have been recognized. Secondarily, the much reduced π bonding between nickel and the ketones tends to augment the initial driving force—the double population of the xy orbital—by ca. 2000 cm^{-1} of increased LFSE.

For the analogous copper(II) complex, we now place the extra electron of the d^9 configuration in the $x^2 - y^2$ orbital. Not only should the Cu–O bond lengths be long, and indeed they are very similar to the Ni–O ones, but so also should the copper–nitrogen bonds which involve σ bonding predominantly with the $x^2 - y^2$ orbital; the observed bond lengths,[2] in Table III, confirm this prediction. We concur with Palenik and Westers' suggestion[5] that the increased in-plane bond lengths diminish nonbonded repulsions with the axial ligands, so permitting the closer approach of the latter to the central metal as we pass to heavier elements in this transition period.

Conclusion

In this and the previous paper[1] we have quantitatively reproduced the complete single-crystal principal paramagnetic susceptibilities and some spectral features of these seven-coordinate DAPSC complexes of iron(II), cobalt(II), and nickel(II). The angular overlap parameters deduced from these studies have been determined reasonably sensitively and all appear chemically comprehensible. They reflect on the essential "normality" of the metal–pyridine, –imine, –aquo, and –chloro σ interactions, again describe only weak π interaction with the pyridine group but substantially greater with the formally sp^2 hybridized imine groups, and concur with the notion of greater π donation from the chlorine axial ligand than from the waters. In all four complexes we observe a relatively weak σ donation from the keto groups of the semicarbazones which decreases markedly on decreasing the acceptor property of the metal d_{xy} orbital caused by the formal electron filling of this orbital as iron(II) or cobalt(II) are replaced by nickel(II), and the consequent rationale of the increased metal–keto bond lengths immediately provides understanding of the bond lengths observed in the analogous copper(II) complex. These primary conclusions derive from the way the spectra and magnetism of these compounds are sensitive to the degree of metal–keto π interactions, which heuristically may be envisaged as consequential upon the change in bond lengths following the change in σ-acceptor property of the central metal.

Acknowledgment. We thank Professor J. Lewis for his interest and helpful discussions and Mr. L. Hanton for help with recording the spectrum of the nickel complex.

Registry No. $[Fe(DAPSC)Cl,H_2O]^+Cl^-$, 71049-92-8; $[Ni(DAPSC)(H_2O)_2]^{2+}(NO_3^-)_2$, 54326-90-8.

References and Notes

(1) M. Gerloch, I. Morgenstern-Badarau, and J. P. Audiere, *Inorg. Chem.*, preceding paper in this issue.
(2) G. J. Palenik and D. W. Wester, *J. Am. Chem. Soc.*, **96**, 7565 (1974).
(3) G. J. Palenik and D. W. Wester, *J. Am. Chem. Soc.*, **95**, 6505 (1973).
(4) G. J. Palenik, personal communication.
(5) G. J. Palenik and D. W. Wester, *Inorg. Chem.*, **17**, 864 (1978).
(6) M. Gerloch, *Prog. Inorg. Chem.*, in press.
(7) M. Gerloch and I. Morgenstern-Badarau, *J. Chem. Soc., Dalton Trans.*, 1619 (1977).
(8) M. Gerloch and R. F. McMeeking, *J. Chem. Soc., Dalton Trans.*, 2443 (1975).
(9) J. E. Davies, M. Gerloch, and D. J. Phillips, *J. Chem. Soc., Dalton Trans.*, in press.
(10) The inequality of the Ni–O bond lengths does not seem explicable simply in terms of a Jahn–Teller splitting of the xy and $x^2 - y^2$ orbitals, as the degeneracy of these two orbitals is raised directly by the dissimilar σ contributions from the set of nitrogen donors compared with the oxygens. If the splitting between these orbitals found for the cobalt systems were sufficiently small that the Jahn–Teller effect should operate on addition of the further electron for nickel(II), a change (weakening) of both Ni–O bond lengths equally would, as shown in Figure 5, be sufficient to raise the degeneracy further; it does not seem obvious why unsymmetrical lengthening of the Ni–O bonds should be more or less advantageous. However, with bonds as long and weak as these, small variations in nonbonded interactions, intra- or intermolecular in origin, are expected to have marked effects as observed in many "octahedral" copper(II) complexes.